

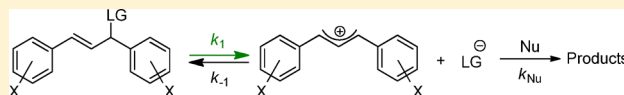
Electrofugalities of 1,3-Diarylallyl Cations

Konstantin Troshin and Herbert Mayr*

Department Chemie, Ludwig-Maximilians-Universität München, Butenandtstrasse 5-13 (Haus F), 81377 München, Germany

S Supporting Information

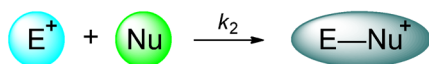
ABSTRACT: Heterolysis rate constants k_1 of differently substituted 1,3-diarylallyl halides and carboxylates have been determined in various solvents. The linear free energy relationship $\log k_1 = s_f(N_f + E_f)$ was found to predict the heterolysis rates ($\log k_1$) of 1,3-diarylallyl derivatives with a standard deviation of 0.26, corresponding to a factor of 1.82 in k_1 , and maximum deviation in k_1 of a factor of 5. Some systematic deviations are evident, however. Thus, 1,3-diarylallyl carboxylates always react faster and 1,3-diarylallyl chlorides always react more slowly than calculated by the quoted correlation equation when both types of leaving groups were used to determine the electrofugality parameters E_f . As 1,3-diarylallyl cations are generated faster in solvolysis reactions and also react faster with nucleophiles than benzhydrylium ions of similar thermodynamic stabilities, i.e., Lewis acidities, one can conclude that the reactions involving 1,3-diarylallyl cations proceed with lower intrinsic barriers than those involving benzhydrylium ions. The electrofugality parameters E_f of 1,3-diarylallylium ions determined in this work were combined with the electrophilicity parameters E of the corresponding cations as well as with the results on ion pair dynamics reported in preceding papers for generating the full mechanistic spectrum of 1,3-diarylallyl solvolyses.



INTRODUCTION

In recent work, we have demonstrated that the rates of the reactions of electrophiles with nucleophiles as well as the rates of the reverse reactions, e.g., heterolyses of covalent esters,¹ follow the three-parameter linear free energy relationships 1 and 2, respectively.

Electrophile-nucleophile combinations



$$\log k_2 = s_N(N + E) \quad (1)$$

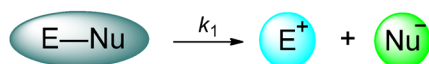
k_2 : second-order rate constant at 20 °C / M⁻¹s⁻¹

s_N : solvent-dependent nucleophile-specific sensitivity parameter

N : solvent-dependent nucleophilicity parameter

E : electrophilicity parameter

Heterolysis reactions



$$\log k_1 = s_f(N_f + E_f) \quad (2)$$

k_1 : first-order rate constant at 25 °C / s⁻¹

s_f : solvent-dependent nucleofuge-specific sensitivity parameter

N_f : solvent-dependent nucleofugality parameter

E_f : electrofugality parameter

A series of variously substituted benzhydrylium ions were chosen as reference electrophiles and electrofuges for the

construction of comprehensive nucleophilicity and electrofugality² as well as nucleofugality and electrofugality³ scales.

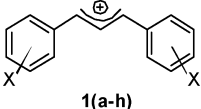
Because of the occurrence of allylic rearrangements, solvolyses of allyl derivatives were of particular importance for the development of the mechanistic understanding of aliphatic nucleophilic substitutions.⁴ Pioneering studies by Goering brought new insights into structure and reactivities of ion pairs;⁵ however, the mechanistic investigations were limited by the analytical methods available at that time. In a recent study, we employed the capability of modern HPLC to clarify the ion-pair dynamics during the solvolyses of unsymmetrical 1,3-diarylallyl derivatives and showed how eq 1 can be used to predict the extent of external and internal return during solvolysis.⁶ We also demonstrated that the rates of the reactions of 1,3-diarylallyl cations **1a–h** with a manifold of π - and n -nucleophiles in various solvents can be described by eq 1, and we determined the E parameters of the 1,3-diarylallyl cations **1a–h** which are depicted in Table 1.⁷ We now studied the solvolysis rates of various derivatives of cations **1a–h** in order to determine their electrofugality parameters E_f according to eq 2. We will subsequently compare the electrofugalities E_f with the corresponding electrophilicity parameters E in order to elucidate general relationships between electrophilicities and electrofugalities.

RESULTS AND DISCUSSION

Synthesis of the Substrates. The (E)-1,3-diarylallyl chlorides **1(a–e)-Cl**, the bromide **1a-Br**, the 4-nitrobenzoates **1(c,e,f)-OPNB**, and the 3,5-dinitrobenzoates **1(b–f)-ODNB** were synthesized from the corresponding alcohols (obtained as

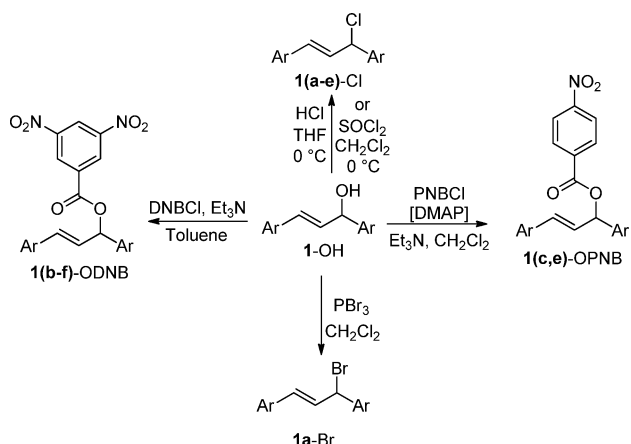
Received: January 2, 2013

Published: January 31, 2013

Table 1. 1,3-Diarylallyl Cations 1a–h and Their Electrophilicity Parameters *E* (from Ref 7)


	X	<i>E</i>
1a	<i>m,m</i> -F ₂	6.11
1b	<i>m</i> -F	4.15
1c	<i>p</i> -Br	2.85
1d	<i>p</i> -Cl	2.69
1e	H	2.70
1f	<i>p</i> -Me	1.23
1g	<i>p</i> -OMe	-1.45
1h	<i>p</i> -NMe ₂	-7.50

described in ref 7) by using standard procedures as depicted in Scheme 1.

Scheme 1. Syntheses of the Substrates 1(a–f)-LG^a

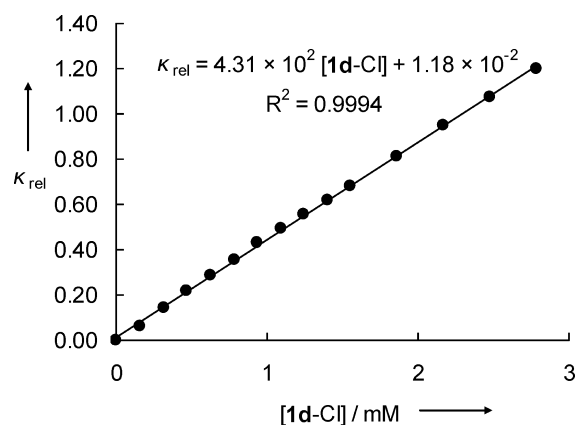
^aAbbreviations used: DNB = 3,5-dinitrobenzoyl, PNB = 4-nitrobenzoyl, DMAP = 4-dimethylaminopyridine.

The highly reactive (*E*)-1,3-diarylallyl acetates and benzoates 1(g,h)-OAc and 1(g,h)-OBz were generated in solution by mixing the corresponding (*E*)-1,3-diarylallylium tetrafluoroborates (1(g,h)-BF₄) with an excess of the tetrabutylammonium carboxylates until colorless solutions were obtained.

Kinetic Experiments. As the bis(dimethylamino)-substituted cation 1h formed by solvolysis of 1h-OAc or 1h-OBz in aqueous acetone or acetonitrile is stable under the reaction conditions, the solvolyses of these substrates were followed spectrophotometrically at 704 nm (absorption maximum of 1h). All other reactions were followed conductimetrically using conventional ($k_1 < 0.15 \text{ s}^{-1}$) or stopped-flow techniques. Because of the direct proportionality between conductivity and concentration of the acid or salt (in the presence of amine additives) produced during the solvolysis (Figure 1 and Figure S2 of the Supporting Information), the rate constants k_{obs} were obtained by fitting the time-dependent conductivity (κ_t) to the monoexponential function (3).

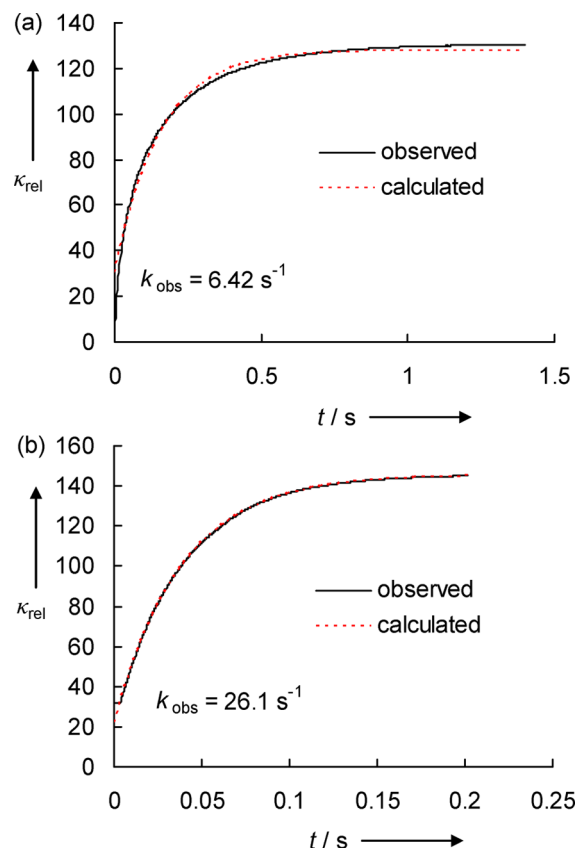
$$\kappa_t = \kappa_{\infty}(1 - e^{-k_{\text{obs}}t}) + C \quad (3)$$

As the carboxylic acids produced during solvolyses of diarylallyl carboxylates are only partially dissociated in aqueous

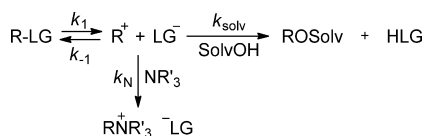
**Figure 1.** Linear dependence of the relative conductivity κ_{rel} on the concentration of HCl (generated by solvolysis of 1d-Cl in 60% aq acetone (60A40W)), 25 °C.

acetone and acetonitrile solutions, solvolyses of such substrates were performed in the presence of amines or pyridines to ensure complete dissociation of the generated acids which resulted in a linear dependence of κ on the acid concentration.

In many cases, kinetics, which did not follow monoexponential functions (Figure 2a), were observed due to recombination of the carbocation with the anion of the leaving group (k_{-1} , Scheme 2, common ion rate depression).

**Figure 2.** Increase of conductivity during solvolyses of 1,3-diphenylallyl chloride (1e-Cl) in 90% aq acetonitrile (90AN10W) at 25 °C (a) in the absence of added nucleophiles and (b) in the presence of 0.30 M 4-(*N,N*-dimethylamino)pyridine (DMAP).

Scheme 2. Simplified Solvolysis Scheme



The addition of strong neutral nucleophiles (amines, pyridines, phosphines) was shown to suppress common ion rate depression in benzhydryl halide solvolyses, as these nucleophiles rapidly trap the carbenium ions without attacking the precursor substrates in an S_N2 mode.⁸ In order to confirm that the solvolysis rate constants determined in this work reflect the rates of the heterolysis step, several measurements with increasing concentrations of amines were performed. In cases where the kinetics in the absence or the presence of small concentrations of amines did not follow monoexponential functions, estimates of k_{obs} were derived from the best fit of the experimental curve to the exponential function (eq 3) as depicted in Figure 2a.

The quality of the monoexponential fits improved with increasing concentration of amines (Figure 2b), and the values of k_{obs} reached a plateau after an initial increase (Figure 3). The

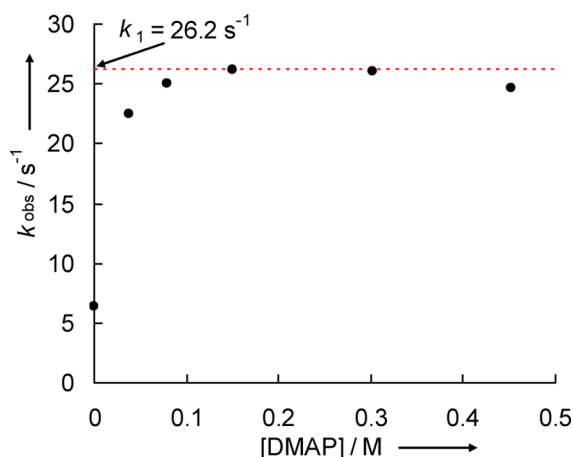


Figure 3. Observed rate constants k_{obs} for the heterolysis of **1e-Cl** at variable concentrations of 4-(*N,N*-dimethylamino)pyridine (DMAP) in 90% aq acetonitrile (90AN10W) at 25 °C.

nonlinearity of the k_{obs} vs [Nu] plots excludes the operation of S_N2 or S_N2' mechanisms, and the plateaus correspond to the concentrations where the common ion rate depression is completely suppressed because the carbocations generated during the heterolysis step are completely trapped by the solvent or by amines before they can recombine with the leaving group. The values of k_{obs} at the plateaus, therefore, correspond to the heterolysis rate constants k_1 . The slight dependence of the heights of the plateaus on the nature of the added nucleophiles,^{8,9} is negligible for the determination of the E_f values considering the logarithmic character of eq 2.

For the solvolyses of the 1,3-diaryllallyl chlorides **1(a-e)-Cl** in aqueous acetonitrile the amount of common ion return depends on the electrophilicities of the carbocations and the content of water in the solvent, as previously found for solvolyses of benzhydryl⁸ and trityl⁹ derivatives. The occurrence of common ion return can be rationalized on the basis of eq 1. The second-order rate constants for the reactions of Cl^- in 60% aq acetonitrile ($N = 12.00$, $s_N = 0.60$)¹⁰ with the

1,3-diaryllallyl cations **1** (E from Table 1) can be calculated by eq 1 to be in the range of $(6.5\text{--}8.1) \times 10^8 \text{ M}^{-1} \text{ s}^{-1}$ for **1c-e** and to be diffusion-controlled ($\approx 5 \times 10^9 \text{ M}^{-1} \text{ s}^{-1}$) for the reactions with **1a,b**. At $[\text{I-Cl}]_0 = 10^{-2} \text{ M}$, a typical initial substrate concentration for stopped-flow experiments in this work, one would expect the effective recombination rate constants $k_{-1}[\text{Cl}^-]$ at 50% conversion ($[\text{Cl}^-] = 5 \times 10^{-3} \text{ M}$) to be approximately $(3.3\text{--}4.1) \times 10^6 \text{ s}^{-1}$ for **1c-e** and ca. $2.5 \times 10^7 \text{ s}^{-1}$ for **1a,b**. These values are of similar magnitude as the calculated first-order rate constants for the reactions of **1c-e** with water in 60% aq acetonitrile ($N = 5.05$, $s_N = 0.89$)¹¹ $k_{\text{solv}} = (7.7\text{--}11) \times 10^6 \text{ s}^{-1}$; common ion rate depression is, therefore, observed in these cases. Lowering the water concentration in the solvent will increase the nucleophilicity of the anionic leaving group (N value of Cl^- is 13.30 in 80% aqueous acetonitrile) and slightly decrease k_{solv} (for 90% aq acetonitrile, $N = 4.56$, $s_N = 0.94$). Both factors result in an increase of the k_{-1}/k_{solv} ratio and explain why common ion rate depression increases with decreasing water concentration in the solvent. The same reasoning also holds for aqueous acetone of variable water concentration.

On the other hand, the diffusionally limited reactions of **1a,b** with Cl^- ($5 \times 10^{-3} \text{ M}$) are significantly slower than the reactions of these cations with the solvent, $k_{\text{solv}}(\mathbf{1a}) = 8.6 \times 10^9 \text{ s}^{-1}$ and $k_{\text{solv}}(\mathbf{1b}) = 1.5 \times 10^8 \text{ s}^{-1}$; the absence of common ion rate depression in the solvolyses of **1(a,b)-Cl** can thus be explained.

As the typical substrate concentrations for the investigations of solvolyses of **1(c-g)-OCOR** with conventional conductimetry were at least 10 times lower than those used to follow the solvolyses of **1(c-e)-Cl** with stopped-flow techniques, and the nucleophilicities of the carboxylate anions are generally lower than those of the halide anions,^{2b} the extent of common ion return observed for solvolyses of **1(c-g)-OCOR** was much smaller than that for **1(c-e)-Cl**.

By multiplication of the second order rate constant $k_2 = 10^3 \text{ M}^{-1} \text{ s}^{-1}$ calculated for the reaction of the bis(dimethylamino)-substituted cation **1h** with acetate anion in 80% aq acetone using eq 1 ($E = -7.50$, $N = 12.50$, $s_N = 0.60$) with 10^{-3} M (the upper limit of $[\text{Bu}_4\text{NOAc}]$ used in solvolyses of **1h-OAc**), one obtains a first-order recombination rate constant of $k_{\text{eff}} = 1 \text{ s}^{-1}$ which is much smaller than the heterolysis rate constants $k_1 \geq 78 \text{ s}^{-1}$ for **1h-OAc** in aqueous acetone and acetonitrile (Table 2). Therefore, the concentration of Bu_4NOAc , which was mixed with **1h-BF₄** in order to generate an anhydrous solution of **1h-OAc**, did not have an effect on the heterolysis rate constants listed in Table 2, which were observed when the solutions of **1h-OAc** in acetone or acetonitrile were mixed with water. The same is true for heterolyses of **1h-OBz**.

Winstein–Grunwald Analysis. The values of $\log k_1$ for the solvolyses of **1-Cl** in various solvents correlate well with the corresponding solvent ionizing powers Y_{Benzyl} ¹² (Figure 4). The m values given in Figure 4 are slightly smaller than those for solvolyses of benzhydryl chlorides of similar reactivity in aqueous acetone and acetonitrile ($m = 0.96$ for diphenylmethyl chloride ($E_f = -6.03$), $m = 0.93$ for bis(*p*-tolyl)methyl chloride ($E_f = -3.44$)).¹³

Increasing cation stability (ca. 3 orders of magnitude in electrophilicity) does not change the m values significantly, and their magnitudes indicate a high carbocation character in the transition states of the heterolyses of **1(a-e)-Cl** in aqueous acetone and acetonitrile. This conclusion can also be reached by consideration of the rate constants of the reactions of the

Table 2. Heterolysis Rate Constants k_1 of (*E*)-1,3-Diaryllallyl Halides and Carboxylates (at 25 °C)

electrofuge	E_f^{a}	nucleofuge	solvent ^b	N_f	s_f	k_1/s^{-1}	k_{calc}^c	k_1/k_{calc}		
1a (X = <i>m,m</i> -F ₂)	-5.07	Cl ⁻	90A10W	1.14	1.11	8.95×10^{-5}	4.34×10^{-5}	2.06		
			80A20W	2.03	1.05	7.44×10^{-4}	6.43×10^{-4}	1.16		
		Cl ⁻	60A40W	3.30	0.97	1.95×10^{-2}	1.92×10^{-2}	1.02		
			90AN10W	2.23	1.08	8.37×10^{-4}	8.57×10^{-4}	0.98		
		Cl ⁻	80AN20W	2.96	1.00	6.86×10^{-3}	7.76×10^{-3}	0.88		
			60AN40W	3.84	0.96	6.32×10^{-2}	6.59×10^{-2}	0.96		
		Br ⁻	90A10W	2.29	1.01	1.35×10^{-3}	1.56×10^{-3}	0.87		
			80A20W	3.01	0.90	1.03×10^{-2}	1.40×10^{-2}	0.74		
		Br ⁻	60A40W	<i>d</i>	<i>d</i>	1.95×10^{-1}				
			90AN10W	<i>d</i>	<i>d</i>	1.26×10^{-2}				
			80AN20W	<i>d</i>	<i>d</i>	8.83×10^{-2}				
			60AN40W	5.23	0.99	5.54×10^{-1}	1.44	0.38		
			Br ⁻	100E	2.93	0.93	1.81×10^{-2}	1.02×10^{-2}	1.77	
1b (X = <i>m</i> -F)	-2.70	-ODNB ^e	80A20W	-2.34	1.10	1.05×10^{-5}	2.86×10^{-6}	3.67		
			60A40W	-2.20	0.90	7.31×10^{-5}	3.89×10^{-5}	1.88		
		-ODNB	60AN40W	-2.06	0.97	1.03×10^{-4}	2.41×10^{-5}	4.27		
			Cl ⁻	90A10W	1.14	1.11	6.38×10^{-3}	1.86×10^{-2}	0.34	
		Cl ⁻	80A20W	2.03	1.05	9.96×10^{-2}	1.98×10^{-1}	0.50		
			60A40W	3.30	0.97	2.91	3.82	0.76		
		Cl ⁻	90AN10W	2.23	1.08	1.29×10^{-1}	3.11×10^{-1}	0.41		
			60AN40W	3.84	0.96	8.97	1.24×10^1	0.72		
		1c (X = <i>p</i> -Br)	-1.37	-OPNB ^f	60A40W	-2.79	1.11	7.76×10^{-5}	2.41×10^{-5}	3.22
					80AN20W	-3.41	0.98	2.77×10^{-5}	2.07×10^{-5}	1.34
-OPNB	60AN40W			-3.30	0.91	1.18×10^{-4}	5.63×10^{-5}	2.10		
	-ODNB			90A10W	-2.68	1.13	2.68×10^{-5}	2.65×10^{-5}	1.01	
-ODNB	60A40W			-2.20	0.90	1.08×10^{-3}	6.12×10^{-4}	1.76		
	Cl ⁻			90A10W	1.14	1.11	3.01×10^{-1}	5.56×10^{-1}	0.54	
Cl ⁻	80A20W			2.03	1.05	3.04	4.93	0.62		
	60A40W			3.30	0.97	4.92×10^1	7.45×10^1	0.66		
Cl ⁻	90AN10W			2.23	1.08	4.47	8.49	0.53		
	80AN20W			2.96	1.00	2.40×10^1	3.89×10^1	0.62		
1d (X = <i>p</i> -Cl)	-1.23	-ODNB	80A20W	-2.34	1.10	2.30×10^{-4}	1.18×10^{-4}	1.95		
			60A40W	-2.20	0.90	1.79×10^{-3}	8.18×10^{-4}	2.19		
		-ODNB	60AN40W	-2.06	0.97	1.75×10^{-3}	6.44×10^{-4}	2.72		
			Cl ⁻	90A10W	1.14	1.11	4.10×10^{-1}	7.95×10^{-1}	0.52	
		Cl ⁻	80A20W	2.03	1.05	4.34	6.92	0.63		
			90AN10W	2.23	1.08	6.01	1.20×10^1	0.50		
		Cl ⁻	80AN20W	2.96	1.00	3.34×10^1	5.37×10^1	0.62		
1e (X = H)	-0.46	-OPNB	80A20W	-3.40	1.16	6.40×10^{-5}	3.33×10^{-5}	1.92		
			60A40W	-2.79	1.11	6.59×10^{-4}	2.47×10^{-4}	2.67		
		-OPNB	60AN40W	-3.30	0.91	7.86×10^{-4}	3.79×10^{-4}	2.07		
			-ODNB	80A20W	-2.34	1.10	1.06×10^{-3}	8.32×10^{-4}	1.27	
		-ODNB	60A40W	-2.20	0.90	6.87×10^{-3}	4.04×10^{-3}	1.70		
			-ODNB	90AN10W	<i>d</i>	<i>d</i>	8.61×10^{-4}			
		-ODNB	80AN20W	<i>d</i>	<i>d</i>	2.54×10^{-3}				
			-ODNB	60AN40W	-2.06	0.97	7.36×10^{-3}	3.59×10^{-3}	2.05	
		Cl ⁻	90A10W	1.14	1.11	1.93	5.69	0.34		
			80A20W	2.03	1.05	1.96×10^1	4.45×10^1	0.44		
		Cl ⁻	90AN10W	2.23	1.08	2.62×10^1	8.16×10^1	0.32		
			80AN20W	2.96	1.00	1.66×10^2	3.16×10^2	0.53		
		1f (X = <i>p</i> -Me)	1.18	-OPNB	80A20W	-3.40	1.16	1.74×10^{-3}	2.66×10^{-3}	0.65
					60A40W	-2.79	1.11	2.04×10^{-2}	1.63×10^{-2}	1.25
-OPNB	90AN10W			<i>d</i>	<i>d</i>	2.16×10^{-3}				
	-OPNB			80AN20W	-3.41	0.98	6.75×10^{-3}	6.53×10^{-3}	1.03	
-OPNB	60AN40W			-3.30	0.91	2.19×10^{-2}	1.18×10^{-2}	1.86		
	-ODNB			90A10W	-2.68	1.13	1.26×10^{-2}	2.02×10^{-2}	0.62	
-ODNB	80A20W			-2.34	1.10	4.30×10^{-2}	5.30×10^{-2}	0.81		
	60A40W			-2.20	0.90	1.42×10^{-1}	1.21×10^{-1}	1.17		
-ODNB	90AN10W			<i>d</i>	<i>d</i>	3.51×10^{-2}				
	80AN20W			<i>d</i>	<i>d</i>	8.21×10^{-2}				
-ODNB	60AN40W	-2.06	0.97	1.92×10^{-1}	1.40×10^{-1}	1.37				

Table 2. continued

electrofuge	E_f^a	nucleofuge	solvent ^b	N_f	s_f	k_1/s^{-1}	k_{calc}^c	k_1/k_{calc}
1g (X = <i>p</i> -OMe)	2.87	⁻ OAc	80A20W	-4.73	1.18	5.15×10^{-3}	6.39×10^{-3}	0.81
		⁻ OAc	80AN20W	-4.52	1.11	1.22×10^{-2}	1.47×10^{-2}	0.83
		⁻ OAc	60AN40W	-4.18	1.08	6.90×10^{-2}	3.85×10^{-2}	1.79
		⁻ OBz	80A20W	-4.46	1.17	1.32×10^{-2}	1.38×10^{-2}	0.95
		⁻ OBz	80AN20W	-4.19	1.12	2.97×10^{-2}	3.32×10^{-2}	0.89
1h (X = <i>p</i> -NMe ₂)	6.39	⁻ OAc	80A20W	-4.73	1.18	7.85×10^1	9.09×10^1	0.86
		⁻ OAc	60A40W	-4.05	1.17	4.21×10^{2g}	5.47×10^2	0.77
		⁻ OAc	80AN20W	-4.52	1.11	1.48×10^2	1.19×10^2	1.24
		⁻ OAc	60AN40W	-4.18	1.08	2.81×10^2	2.44×10^2	1.15
		⁻ OBz	80A20W	-4.46	1.17	1.57×10^2	1.81×10^2	0.87
		⁻ OBz	60AN40W	-3.92	1.02	3.31×10^2	3.31×10^2	1.00

^aThe E_f parameters for 1a–h result from the least-squares minimization of $\Delta^2 = \sum(\log k_1 - s_f(N_f + E_f))^2$ which uses the heterolysis rate constants k_1 (this table) and the N_f and s_f parameters of the nucleofuges given in ref 3a and listed in this table. ^bAll solvent compositions are given in vol %, A = acetone, AN = acetonitrile, E = ethanol, W = water. ^cThe values of k_{calc} were obtained using eq 2 and E_f , s_f and N_f parameters listed in this table. ^dThe values of s_f and N_f are not available. ^e-ODNB = 3,5-Dinitrobenzoate. ^f-OPNB = 4-Nitrobenzoate. ^gThis rate constant was not included in the correlation since the heterolysis is too fast to derive a reliable value of k_1 .

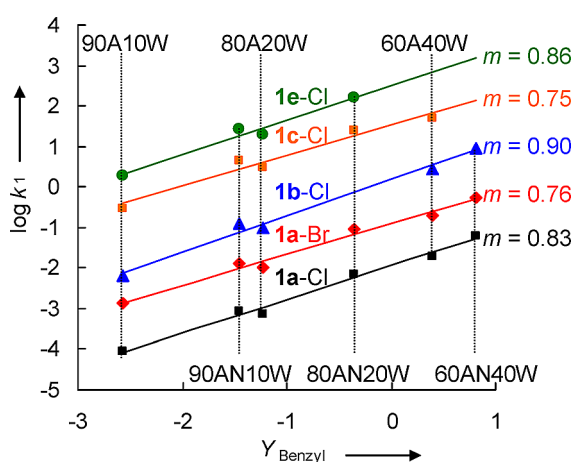


Figure 4. Correlation between the solvolysis rate constants of 1-Hal in acetone/water and acetonitrile/water mixtures (from Table 2) and the corresponding Y_{Benzyl} values.^{12d} The line for 1d-Cl ($m = 0.85$) is not drawn to avoid overlap.

1,3-diaryllallyl cations with Cl^- (principle of microscopic reversibility). As discussed above, 1e and the more reactive carbocations 1a–d react with chloride ions in these solvents with second-order rate constants $k_2 > 7 \times 10^8 \text{ M}^{-1} \text{ s}^{-1}$,

indicating that there is no or only a very small barrier for the ion combination, which is equivalent to a carbocation-like transition states.

A different situation is found for the solvolyses of 1-OCOR. For all carboxylates (plots for 1-ODNB and 1-OPNB are shown in Figure 5), the m values are less than 0.6 and decrease with increasing cation stability, which is most pronounced for the 3,5-dinitrobenzoates.¹⁴ This situation is very similar to that for benzhydryl¹⁵ and trityl⁹ carboxylates, where the m -values of $\text{Ar}_2\text{CH-OCOR}$ and $\text{Ar}_3\text{C-OCOR}$ were reported to decrease steadily with increasing electrofugalities of the carbocations. As in the benzhydryl and trityl series, the low m -values for allyl carboxylates and their decrease with increasing electrofugality can be rationalized by incompletely developed carbocation character in the transition states.^{9,15} It is noteworthy that the m -values of the allyl carboxylates 1-OCOR are larger than those of benzhydryl carboxylates of similar reactivities (Supporting Information), while the solvolysis rates of 1-Cl and 1-Br (Figure 4) are less sensitive to the changes in solvent ionizing power (i.e., smaller m) than those of their benzhydryl analogs.

Hammett Analysis. The heterolysis rates of 1(a–f)-Cl in 90, 80, and 60% aqueous acetone and acetonitrile correlate with the sum of Hammett–Brown's σ^+ parameters¹⁶ (Figure 6 and the Supporting Information). The ρ -values (-3.4 to -3.1) are lower than those for benzhydryl derivatives of comparable

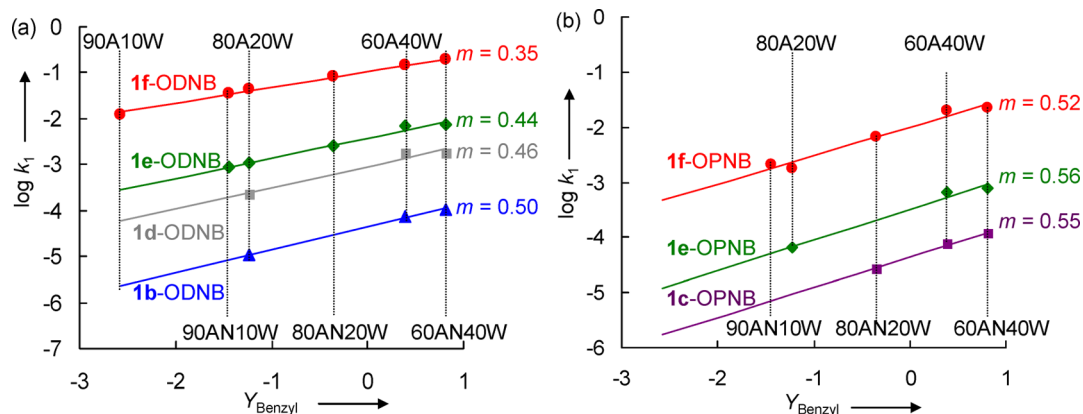


Figure 5. Correlation between the solvolysis rate constants of (a) 1-ODNB and (b) 1-OPNB in acetone/water and acetonitrile/water mixtures (from Table 2) and the corresponding Y_{Benzyl} values.^{12d}

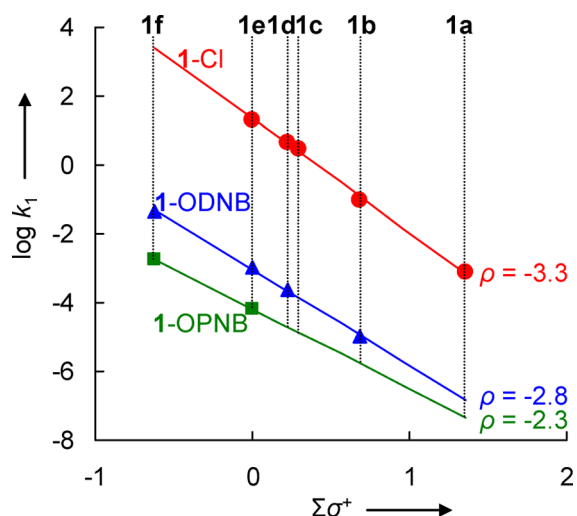


Figure 6. Correlation of the heterolysis rate constants k_1 of 1-LG in 80% aq acetone (80A20W) with the sum of σ^+ parameters of the corresponding aryl substituents (σ^+ from ref 16).

reactivities (-4.2 to -4.1).¹⁷ As in the benzhydryl series,¹⁵ smaller values of ρ are also found for the solvolyses of the allyl 4-nitrobenzoates and 3,5-dinitrobenzoates 1-OCOR ($-2.8 < \rho < -2.3$, Figure 6) again indicating that the transition states of solvolyses of 1,3-diarylallyl chlorides are more carbocation-like than those for 1,3-diarylallyl carboxylate solvolyses.

Determination of the Electrofugality Parameters.

Figure 7 shows that $(\log k_1)/s_f$ for the solvolyses of 1(a–h)-LG correlates linearly with N_f . By minimizing¹⁸ the sum of the

squared deviations $\Delta^2 = \sum(\log k_1 - s_f(N_f + E_f))^2$, one can derive the electrofugality parameters E_f for cations 1a–h listed in Table 2, which correspond to the intercepts on the abscissa of the correlation lines in Figure 7.

Since the use of eq 2 enforces slopes of 1.0 for these correlations, carboxylates are generally above and halides are below the correlation lines, when data for both classes of nucleofuges are used for the correlations. As a consequence one would arrive at better predictions of solvolysis rate constants, when different electrofugality parameters would be employed for allyl carboxylates and allyl halides. For the sake of simplicity and unambiguity we refrain from proliferating the number of parameters and refer to the last column of Table 2 which shows that also with a single set of E_f parameters, experimental and calculated rate constants never deviate by more than a factor of 5. As most rate constants agree much better, we consider these deviations tolerable in view of the fact that the 1,3-diarylallyl cations are covering a reactivity range of 12 orders of magnitude.

Comparison of 1,3-Diarylallyl and Benzhydryl Cations. Depending on the substituents, the electrofugalities of 1,3-diarylallyl cations exceed those of analogously substituted benzhydryl cations by 1.5 to 7.5 orders of magnitude (Figure 8). As for the electrophilicities, the electrofugality range covered by 1,3-diarylallyl ions is smaller than that for analogously substituted benzhydryl systems, and the difference in electrofugalities between the two series decreases with increasing electron-donating abilities of the substituents (Figure 8).

The differences can be explained in the same way as in the case of the electrophilicities:⁷ As the electron-demand of the

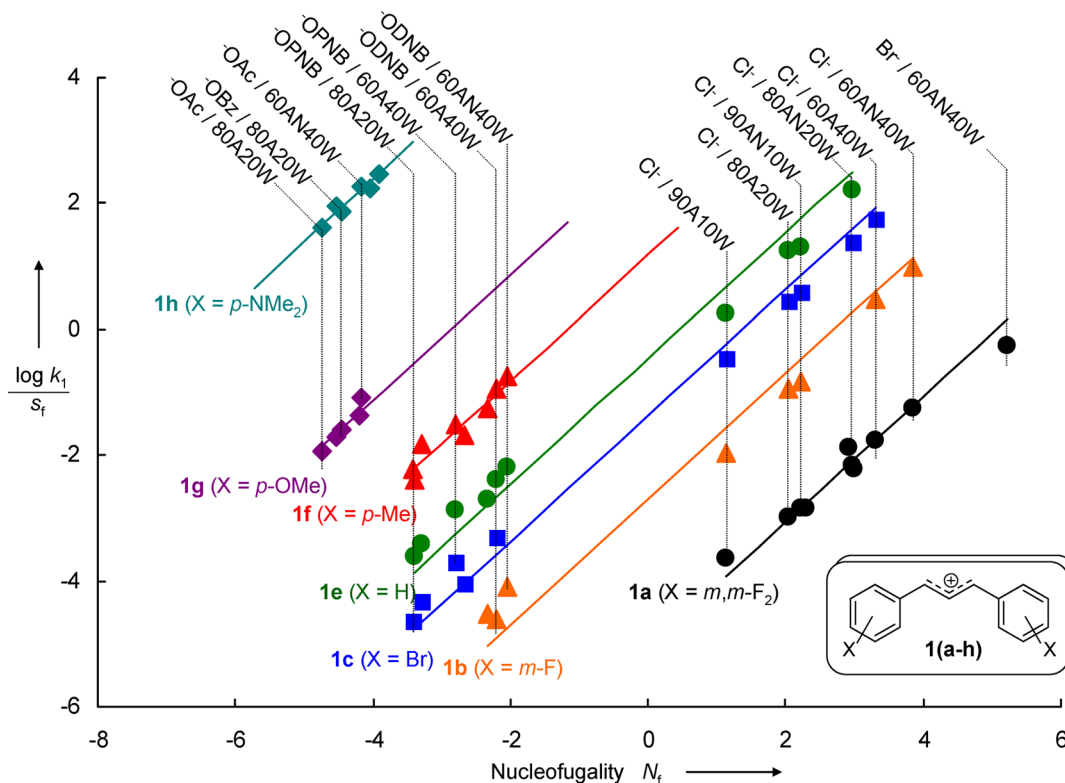


Figure 7. Plot of $(\log k_1)/s_f$ vs N_f for solvolyses of 1(a–h)-LG in various solvents. Abbreviations used for the solvents are A (acetone), AN (acetonitrile), and W (water). All solvent ratios are given in % v/v (i.e., 80A20W means 80% v/v aq acetone). Abbreviations for leaving groups are: ⁻OPNB = 4-nitrobenzoate, ⁻ODNB = 3,5-dinitrobenzoate.

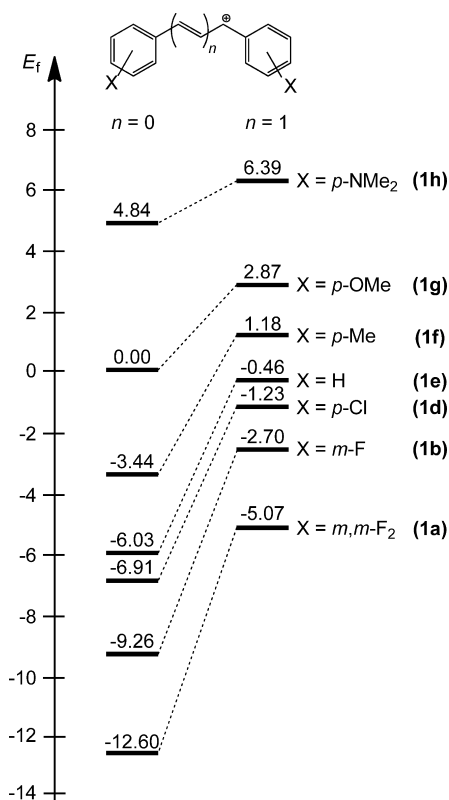


Figure 8. Electrofugalities E_f of **1(a–h)** compared with those of analogously substituted benzhydryl cations.^{3a}

carbenium centers is smaller in the 1,3-diaryllallyl cations due to the charge delocalization over two terminal allylic carbons, substituents have a smaller effect on the rates of their reactions as well as on the rates of their formation.

Figure 9 shows that the electrofugalities of analogously substituted 1,3-diaryllallyl and benzhydryl cations are linearly

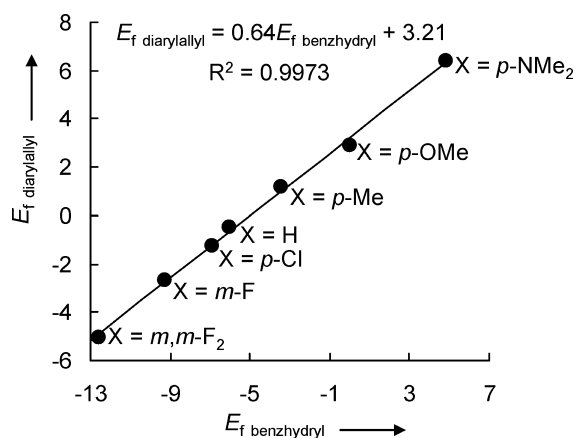
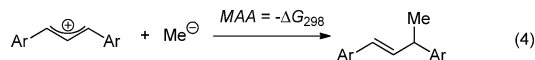


Figure 9. Correlation between the electrofugality parameters E_f of analogously substituted 1,3-diaryllallyl and benzhydryl cations.^{3a}

correlated, as previously reported for the corresponding electrophilicities of these carbocations. The slope of this correlation (0.64) reflects the differences in electron demand between the two series which has already been derived from Figure 8.

As previously reported,⁷ the electrophilicities of the allyl cations **1a–h** increase with increasing methyl anion affinities (MAA, eq 4, red dots in Figure 10a).



Correspondingly, their electrofugalities decrease with increasing methyl anion affinities (red dots in Figure 10b). It is remarkable however, that in both correlations the red dots are above the black squares (benzhydrylium ions) indicating that 1,3-diaryllallyl cations are both better electrophiles (Figure 10a) and better electrofuges (Figure 10b) than benzhydrylium ions of equal methyl anion affinities.¹⁹ One, therefore, can conclude that the reactions of 1,3-diaryllallyl cations proceed with lower intrinsic barriers than the corresponding reactions of benzhydrylium ions, i.e., the heterolyses of the diaryllallyl derivatives **1-LG** (and the reverse ion recombinations) require less reorganization than the corresponding reactions of benzhydryl derivatives. As a consequence of the different intrinsic barriers, **1a–h** are *more electrophilic* than benzhydrylium ions of similar electrofugality and *better electrofuges* than diarylmethyl cations of similar electrophilicity. More specific: The 1,3-bis(*p*-tolyl)allyl cation **1f** is both a better electrophile ($E = 1.23$) and a better electrofuge ($E_f = 1.18$) than the 4,4'-dimethoxybenzhydryl cation ($E = 0$; $E_f = 0$).

This behavior can quantitatively be explained by Marcus theory²⁰ or the related principle of least nuclear motion.²¹ As the formation of 1,3-diaryllallyl cations from covalent precursors as well as their reactions with nucleophiles require less changes of charge densities and related movements of nuclei and solvent molecules than the corresponding processes for benzhydrylium ions of equal Lewis acidities ($\hat{=}$ methyl anion affinities), smaller reorganization energies are needed in the 1,3-diaryllallylium than in the benzhydrylium series.

Let us now analyze how the differences in intrinsic barriers affect the correlations based on eq 2 (Figure 7). When the ion recombination proceeds with diffusion-controlled rate, the activation energy for the heterolytic cleavage (ΔG^\ddagger) equals ΔG^0 of this reaction (principle of microscopic reversibility). This is the case for many bromides and chlorides derived from acceptor-substituted benzhydrylium and 1,3-diaryllallylium ions. As 3,5-dinitrobenzoate and 4-nitrobenzoate anions are less nucleophilic than Cl^- (≥ 100 times), several benzhydrylium ions which have been used to derive the nucleofugality parameters N_f and s_f undergo diffusion-controlled recombinations with Cl^- and activation-controlled reactions with $^-\text{ODNB}$ or $^-\text{OPNB}$. Consequently, the N_f and s_f values of carboxylates embed a larger portion of the intrinsic reactivities of the benzhydrylium ions than the corresponding nucleofuge-specific parameters of Cl^- and Br^- . As the intrinsic reactivities of the 1,3-diaryllallyl cations are higher (i.e., the electrophile-specific contributions to the barriers of their reactions are lower), the experimental heterolysis rates of the corresponding carboxylates are higher than those predicted based on eq 2 using the N_f and s_f parameters based on diarylmethyl cations (see Figure 7). Acceleration of allyl carboxylate solvolysis by the interaction of the carbonyl oxygen with the other allylic terminus cannot be responsible for this deviation, since the contact ion pairs for allyl systems have unsymmetrical structures.²²

Electrophilicity–Electrofugality Relationships. Figure 11, which plots the E_f values of the 1,3-diaryllallyl cations **1a–h** versus their electrophilicity parameters E , demonstrates that,

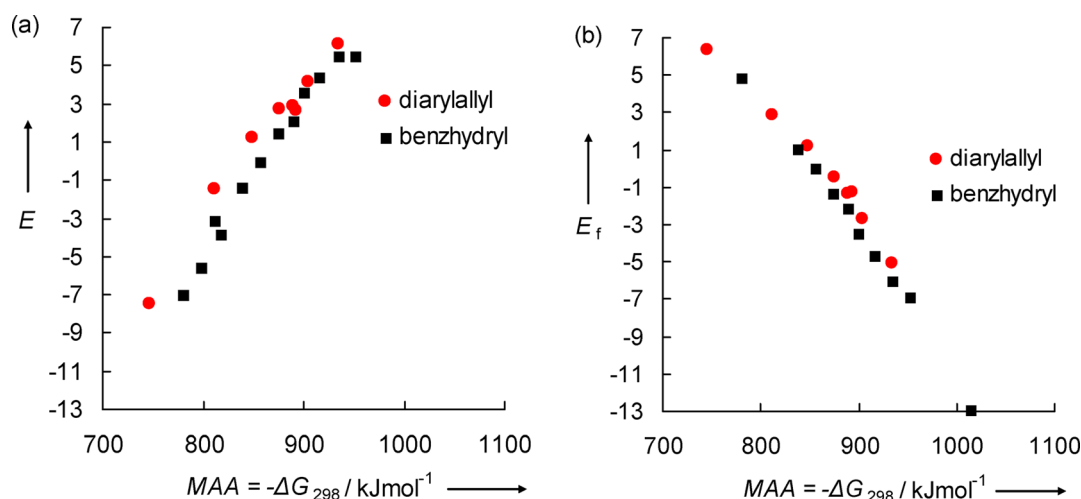


Figure 10. Correlations of (a) electrophilicities and (b) electrofugalities of benzhydryl and 1,3-diaryllallyl cations with their calculated (B3LYP/6-31G(d,p) level of theory) gas-phase methyl anion affinities (MAA) as defined in eq 4.

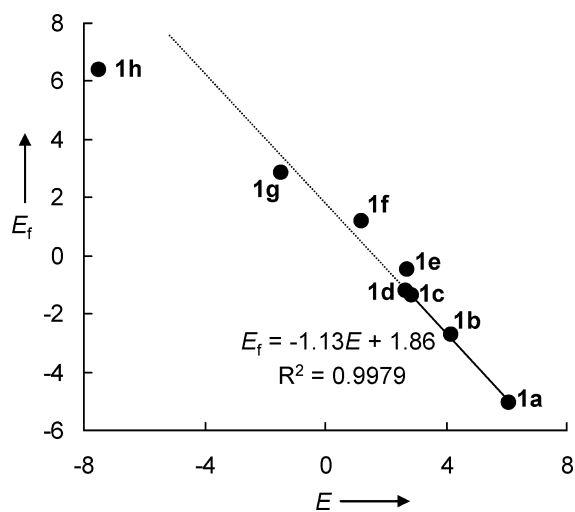


Figure 11. Electrofugality parameters of the cations 1a–h plotted vs their electrophilicities E . The correlation line refers to the acceptor-substituted cations 1a–d.

similar to the situation with benzhydryl^{3a,23} and trityl⁹ systems, the E_f vs E correlation is not linear. The high intrinsic barriers for the reactions involving cations with strong electron donor groups (high reorganization energies) reduce the rates of heterolyses as well as the rates of the reactions with nucleophiles, and this shifts 1h downward and to the left from the extrapolated correlation line in Figure 11.

Parallel S_N1 and S_N2 Mechanisms in Reactions of 1a-Br with Amines. From the dependence of the hydrolysis rates of 1,3-diphenylallyl chloride 1e-Cl in the presence of variable concentrations of DMAP (Figure 3) we derived the operation of an S_N1 mechanism, as k_{obs} became independent of the concentration of DMAP when it exceeded a certain value. A different behavior was observed when 1a-Br was treated with variable amounts of DABCO, piperidine, or morpholine in aqueous acetonitrile and aqueous acetone. As illustrated in Figure 12, one now finds a linear increase of the pseudo-first-order rate constants with increasing amine concentration, indicating S_N2 reactions of the amines with 1a-Br, which are accompanied by an S_N1 process, the rate constant of which (k_1)

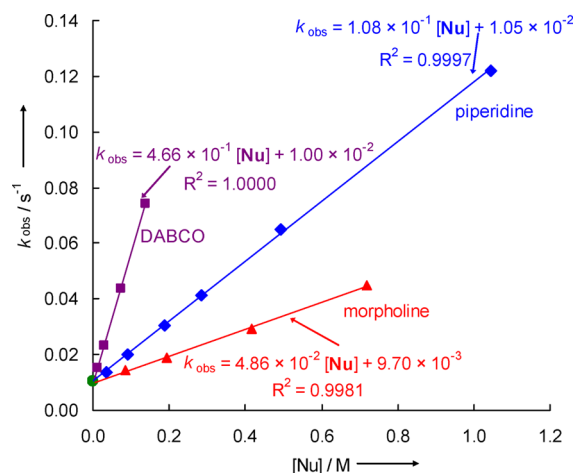


Figure 12. Pseudo-first-order rate constants observed for solvolyses of 1a-Br in 80% aq acetone in the presence of various amine concentrations, 25 °C.

is given by the identical intercepts of the three correlation lines (eq 5).

$$k_{\text{obs}} = k_1 + k_2[\text{amine}] \quad (5)$$

As shown in the Supporting Information, the operation of the rate law (eq 5) has also been observed for the reaction of 1a-Br with these three amines in 90% aqueous acetone as well as in 80% and 90% aq acetonitrile.

Table 3, which summarizes these results, shows that in all solvents, DABCO undergoes the S_N2 reaction approximately 1 order of magnitude faster than morpholine, and piperidine is about two times more reactive than morpholine. A similar reaction sequence for these three amines has previously been reported for their reactions with benzhydryl bromides in DMSO.²⁴

In contrast to the strong solvent effects on the rates of the S_N1 reactions discussed above, the rates of the S_N2 reactions are not or only slightly affected by the solvent polarity. While the nucleophilic substitutions proceed with equal rates in 90% and 80% aqueous acetone, they are even slightly slower in 80% than in 90% aqueous acetonitrile in contrast to the expectations based on the Hughes–Ingold rules, which predict a strong

Table 3. First-Order Rate Constants (s^{-1}) for the Reactions of **1a-Br** with Aqueous Acetone and Acetonitrile (S_N1 solvolysis) and Second-Order Rate Constants ($M^{-1} s^{-1}$) for the Reactions of **1a-Br** with Amines in these Solvents, 25 °C

solvent	k_1/s^{-1}	$k_2 (M^{-1} s^{-1})$		
		DABCO	piperidine	morpholine
90A10W	1.35×10^{-3}	4.97×10^{-1}	1.07×10^{-1}	4.49×10^{-2}
80A20W	1.03×10^{-2}	4.66×10^{-1}	1.08×10^{-1}	4.86×10^{-2}
60A40W	1.95×10^{-1}	$(7.9 \times 10^{-1})^a$	b	b
90AN10W	1.26×10^{-2}	1.23	2.08×10^{-1}	9.40×10^{-2}
80AN20W	8.83×10^{-2}	8.83×10^{-1}	1.46×10^{-1}	b
60AN40W	5.54×10^{-1}	b	$(3.24 \times 10^{-1})^a$	b

^aDue to the uncertainties caused by the fast reaction with the solvent, the k_2 value cannot be precisely determined and should be considered as an estimate. ^bNot determined.

increase of the rates of S_N2 reactions when ions are generated from neutral reactants.²⁵ Obviously, the reduction of the nucleophilicities of the amines by water^{2b} compensates (aqueous acetone) or overcompensates (aqueous acetonitrile) the expected acceleration due to the stabilization of the partially ionic transition states by the solvent.

As **1a** is by far the least stabilized diarylallyl cation of this series, one can explain why amines, which are present as trapping agents to suppress common ion return (Figures 2 and 3), do not undergo S_N2 reactions with other 1,3-diarylallyl derivatives **1(b-f)**-LG.

Changes of Solvolysis Mechanisms of Allyl Derivatives. Figure 13 combines the rate constants for the heterolyses

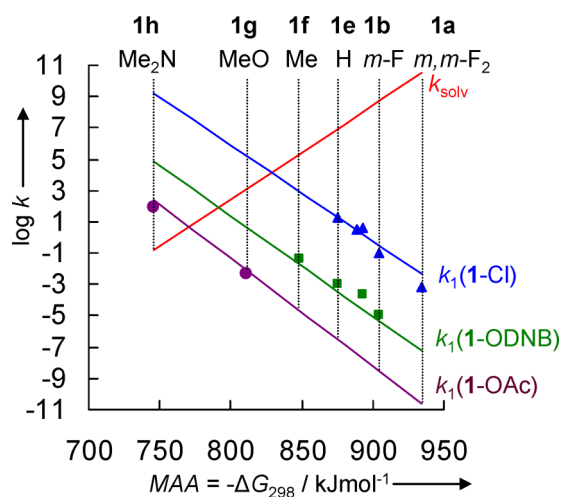


Figure 13. Heterolysis rate constants k_1 for 1-Cl, 1-ODNB, and 1-OAc in 80% aq acetone and of the first-order rate constants k_{solv} for the reactions of **1** with the solvent in correlation with calculated (B3LYP/6-31G(d,p) level of theory) gas-phase methyl anion affinities (MAA) of **1**. Experimentally derived values of k_1 (Table 2) are identified by symbols, and the trend lines correspond to k_1 and k_{solv} calculated for **1(a-h)**-LG and **1a-h** by eqs 2 and 1, respectively.

of allyl derivatives (k_1 of Scheme 2) with the rate constants for the reactions of the allyl cations with 80% aqueous acetone. One can see that the acceptor-substituted allyl chlorides **1(a,b)**-Cl like the unsubstituted (*E*)-1,3-diphenylallyl chloride **1e**-Cl (as well as **1(c,d)**-Cl) follow the typical S_N1 mechanism: slow formation of the carbocation, followed by rapid trapping by the solvent. For $k_1 > k_{solv}$ (i.e., for the left part of Figure 13) the S_N2C^+ mechanism²⁶ is encountered, where a high concentration of an intermediate carbocation is generated in a fast initial step, which is slowly converted into an allyl alcohol in a

subsequent reaction. Crossing of the two correlation lines is expected for an 1,3-diarylallyl chloride with a reactivity between those of the dimethyl- and dimethoxy-substituted 1,3-diarylallyl chlorides **1f**-Cl and **1g**-Cl. From $\log k$ at the point of intersection one can derive that heterolysis of the corresponding 1,3-diarylallyl chloride **1**-Cl as well as solvent capture of the generated carbenium ion occur on the submillisecond time scale, where measurements of the rates of thermal heterolysis are presently not possible.

As the 3,5-dinitrobenzoate anion is a weaker nucleofuge than Cl^- , the correlation line for the heterolysis rate constants of 1-ODNB is lower, and crossing with the k_{solv} graph occurs for allyl cations which are slightly better stabilized than the dimethoxy-substituted system **1g**. Because of the smaller $\log k$ for such 3,5-dinitrobenzoates, the buildup of visually detectable carbocation concentrations can be expected, as previously observed in the benzhydrylium²⁷ and tritylium⁹ series.

Acetate is such a weak leaving group that it was even possible to measure the rate of the heterolytic formation of the highly stabilized dimethylamino-substituted cation **1h** from covalent **1h**-OAc. Though Figure 13 suggests a slow subsequent reaction of **1h** with water, this reaction is highly reversible, and we have observed the formation of the persistent allyl cation **1h** in aqueous acetone (and acetonitrile).

CONCLUSIONS

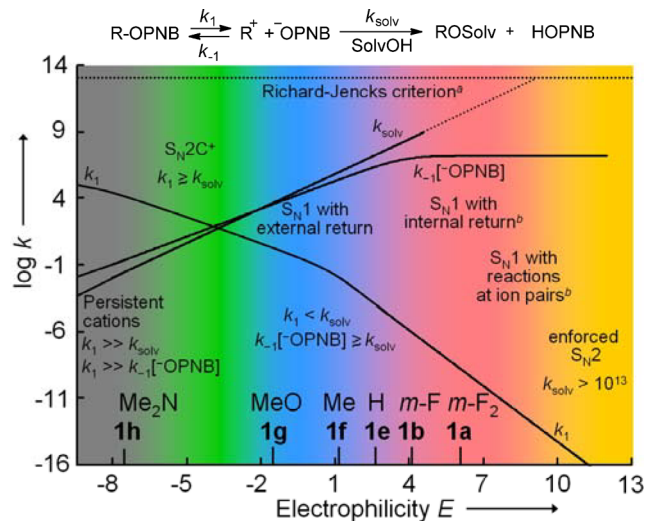
Though the linear free energy relationship $\log k_1 = s_f(N_f + E_f)$ (eq 2) was found to predict heterolysis rates of 1,3-diarylallyl bromides, chlorides, and carboxylates with an accuracy better than factor of 5 from a single set of E_f parameters and a single set of the benzhydrylium-based nucleofuge-specific parameters N_f and s_f , systematic deviations are evident. Thus, the 1,3-diarylallyl carboxylates **1**-OCOR react generally faster, while the 1,3-diarylallyl chlorides **1**-Cl react generally more slowly than predicted when solvolysis rates for both types of leaving groups were used to determine the electrofugality parameters E_f .

As in the benzhydryl^{3a} and trityl⁹ series, solvolyses of 1,3-diarylallyl bromides and chlorides have significantly larger Winstein–Grunwald m -values than carboxylates; this difference has been explained by late and early transition states, respectively. Variation of the substituents in the aromatic rings affects solvolysis rates of 1,3-diarylallyl derivatives significantly less than those of benzhydryl derivatives. As the intrinsic barriers for heterolyses of 1,3-diarylallyl derivatives are lower than those for the corresponding benzhydryl heterolyses, one comes to the conclusion that 1,3-diarylallyl derivatives ionize faster than benzhydryl derivatives of the same electrophilicity E and, at the same time, 1,3-diarylallylium ions

combine faster with nucleophiles than benzhydryl cations of equal electrofugality E_f .

Combination of the electrofugality parameters of 1,3-diaryllallyl ions derived in this work with their electrophilicity parameters E^7 and with the results on ion pair dynamics reported in a preceding publication⁶ allows one to construct the comprehensive solvolysis scheme.

As illustrated in Figure 14, the highly stabilized carbocation **1h** in the left gray range is generated faster by heterolysis of the



^a Ref 28. ^b Ref 6.

Figure 14. Changes of mechanism in solvolyses of 1,3-diaryllallyl 4-nitrobenzoates (**1-OPNB**) in 60% aq acetone ($[\text{OPNB}] = 5 \text{ mM}$).

corresponding covalent ester than it reacts with water or carboxylate ions. As the latter two reactions are highly reversible, **1h** is thermodynamically stable under the reaction conditions. When the stabilization of the carbocations is decreased, one gets into the green S_N2C^+ range,²⁶ where the formation of the carbocation is faster than its reaction with the solvent. Further destabilization of the carbocations (**1g**, **1f**) leads to S_N1 reactions with external (common ion) return, where the consumption of the carbocations is faster than their generation from the covalent precursors, but the rate of recombination with the leaving group LG^- is comparable to the rate of the reaction with the solvent (blue area). If the rate of ion recombination is comparable to that of the diffusional separation of the initially formed ion pairs, one observes internal return (red area) which has extensively been studied with unsymmetrically substituted 1,3-diaryllallyl carboxylates.⁶ The extent of internal return is decreasing again when the electrophilicity of the carbocation is high enough that the solvent can attack at the stage of contact ion pairs (CIPs). An enforced S_N2 reaction can eventually be expected, when the rate constant of the combination of the carbocation with water (k_{solv}) exceeds the vibrational frequency ($\sim 10^{13} \text{ s}^{-1}$, Richard-Jencks criterion²⁸). Equations 1 and 2 can analogously be employed for predicting mechanistic changes in the solvolyses of other series of substrates.

EXPERIMENTAL SECTION

Materials for Kinetic Measurements. Dry ethanol was obtained by distillation of commercially available absolute ethanol from sodium/diethyl phthalate. Doubly distilled water (impedance 18.2 Ω) was obtained from a water purification system. Piperidine (>99%)

and morpholine (>99%) were purchased and distilled prior to use. Acetone (99.8%), acetonitrile (HPLC grade), DMAP (>99%), and DABCO (98%) were purchased and used as received. Details of the kinetic measurements are given in the Supporting Information.

Analyticals. ^1H and ^{13}C NMR chemical shifts are expressed in δ (ppm) and refer to CDCl_3 (δ_{H} 7.26, δ_{C} 77.0), CD_2Cl_2 (δ_{H} 5.32, δ_{C} 54.0), or tetramethylsilane (δ_{H} 0.00, δ_{C} 0.0) as internal standards. The coupling constants are given in Hz. Abbreviations used are: s (singlet), d (doublet), t (triplet), q (quartet), m (multiplet). In case of ^{13}C NMR spectra, these abbreviations refer to the multiplicity in hydrogen decoupled spectra and the hydrogen multiplicity (based on DEPT or HSQC experiments) is shown as CH_3 , CH_2 , CH or C to avoid ambiguity. For the compounds containing no fluorine, the letter "s" is omitted. Assignments of NMR signals are based on the combined analysis of ^1H and ^{13}C NMR, HSQC, HMBC, and COSY spectra.

HRMS in EI mode (70 eV) were determined with sector field detectors. Melting points were determined using a standard melting point unit with gradient of 0.5 $^\circ\text{C}$.

All yields refer to nonoptimized procedures.

(E)-3-Bromo-1,3-bis(3,5-difluorophenyl)prop-1-ene (1a-Br). Compound **1a-Br** was obtained from **1a-OH** (1.03 g, 3.69 mmol) and phosphorus tribromide (420 μL , 1.21 g, 4.48 mmol) using a procedure from ref 29: 708 mg (2.05 mmol, 56%), colorless solid (mp 57.0–59.5 $^\circ\text{C}$). ^1H NMR (CDCl_3 , 300 MHz): δ 5.68 (d, $^3J_{\text{HH}}$ = 7.1 Hz, 1 H, $\text{ArCHCHCH}(\text{Br})\text{Ar}$), 6.49–6.63 (m, 2 H, $\text{ArCHCHCH}(\text{Br})\text{Ar}$), 6.69–6.83 (m, 2 H, H_{Ar}), 6.86–6.98 (m, 2 H, H_{Ar}), 6.98–7.06 ppm (m, 2 H, H_{Ar}). ^{13}C NMR (CDCl_3 , 75 MHz): δ 51.4 (t, J_{CF} = 2.3 Hz, CH), 103.9 (t, J_{CF} = 25.6 Hz, CH), 104.2 (t, J_{CF} = 25.2 Hz, CH), 109.5–109.8 (m, CH), 110.6–111.0 (m, CH), 130.6 (s, CH), 130.9 (t, J_{CF} = 2.9 Hz, CH), 138.9 (t, J_{CF} = 9.6 Hz, C), 143.4 (t, J_{CF} = 9.0 Hz, C), 163.0 (dd, J_{CF} = 248.6, 12.7 Hz, C), 163.2 ppm (dd, J_{CF} = 247.2, 12.9 Hz, C). ^{19}F NMR (CDCl_3 , 282 MHz): δ -109.7 to -109.4 (m), -108.4 to -108.1 ppm (m). HRMS (EI+): calcd 265.0635 ($\text{C}_{15}\text{H}_9\text{F}_4^+(\text{M} - \text{Br}^-)$), found 265.0623.

(E)-3-Chloro-1,3-bis(3,5-difluorophenyl)prop-1-ene (1a-Cl). Compound **1a-Cl** was synthesized as reported in ref 30.

(E)-3-Chloro-1,3-bis(3-fluorophenyl)prop-1-ene (1b-Cl). Compound **1b-Cl** was synthesized from **1b-OH** (530 mg, 2.15 mmol) and thionyl chloride (220 μL , 360 mg, 3.03 mmol) following the protocol described in ref 29: 378 mg (1.26 mmol, 58%), colorless oil. ^1H NMR (CDCl_3 , 400 MHz): δ 5.60 (d, $^3J_{\text{HH}}$ = 7.7 Hz, 1 H, $\text{ArCHCHCH}(\text{Cl})\text{Ar}$), 6.46 (dd, $^3J_{\text{HH}}$ = 15.6, 7.7 Hz, 1 H, $\text{ArCHCHCH}(\text{Cl})\text{Ar}$), 6.60 (d, $^3J_{\text{HH}}$ = 15.6 Hz, 1 H, $\text{ArCHCHCH}(\text{Cl})\text{Ar}$), 6.93–6.99 (m, 1 H, H_{Ar}), 6.99–7.06 (m, 1 H, H_{Ar}), 7.06–7.39 ppm (m, 6 H, H_{Ar}). ^{13}C NMR (CDCl_3 , 101 MHz): δ 62.3 (d, J_{CF} = 2.0 Hz, CH), 113.3 (d, J_{CF} = 22.3 Hz, CH), 114.5 (d, J_{CF} = 22.7 Hz, CH), 115.2 (d, J_{CF} = 21.4 Hz, CH), 115.5 (d, J_{CF} = 21.2 Hz, CH), 122.8 (d, J_{CF} = 2.8 Hz, CH), 122.9 (d, J_{CF} = 3.0 Hz, CH), 129.7 (d, J_{CF} = 0.5 Hz, CH), 130.1 (d, J_{CF} = 8.4 Hz, CH), 130.3 (d, J_{CF} = 8.3 Hz, CH), 131.4 (d, J_{CF} = 2.6 Hz, CH), 137.9 (d, J_{CF} = 7.7 Hz, C), 142.4 (d, J_{CF} = 7.2 Hz, C), 162.8 (d, J_{CF} = 247.2 Hz, C), 163.0 ppm (d, J_{CF} = 245.9 Hz, C). HRMS (EI+): calcd 264.0512 ($\text{C}_{15}\text{H}_{11}\text{ClF}_2$), found 264.0505.

Compounds **1c-Cl** and **1e-Cl** were synthesized as described in ref 7.

(E)-3-Chloro-1,3-bis(4-chlorophenyl)prop-1-ene (1d-Cl). Compound **1d-Cl** was synthesized from **1d-OH** (487 mg, 1.74 mmol) and concentrated hydrochloric acid (1 mL) following the protocol described in ref 31: 344 mg (1.16 mmol, 66%), colorless solid (mp 77.5–80.0 $^\circ\text{C}$). ^1H NMR (CDCl_3 , 300 MHz): δ 5.59 (d, 1 H, $^3J_{\text{HH}}$ = 7.4 Hz, $\text{ArCHCHCH}(\text{Cl})\text{Ar}$), 6.44 (dd, $^3J_{\text{HH}}$ = 15.7, 7.4 Hz, 1 H, $\text{ArCHCHCH}(\text{Cl})\text{Ar}$), 6.56 (d, $^3J_{\text{HH}}$ = 15.7 Hz, 1 H, $\text{ArCHCHCH}(\text{Cl})\text{Ar}$), 7.22–7.43 ppm (m, 8 H, H_{Ar}). ^{13}C NMR (CDCl_3 , 75 MHz): δ 62.6 (CH), 128.0 (CH), 128.7 (CH), 128.8 (CH), 128.9 (CH), 129.2 (CH), 131.2 (CH), 134.1 (2 \times C), 134.3 (C), 138.5 ppm (C). HRMS (EI+): calcd 296.9999 ($\text{C}_{15}\text{H}_{11}\text{Cl}_3 + \text{H}^+$), found 296.9987.

General Procedure for Synthesis of 1,3-Diaryllallyl 3,5-Dinitrobenzoates (1-ODNB). 3,5-Dinitrobenzoyl chloride (1–2 equiv) was added to a stirred solution of the corresponding alcohol **1-OH** (1 equiv) and triethylamine (1.2 equiv with respect to DNBCl) in toluene. After 12 h of stirring, the reaction mixture was quenched

with 0.1 M aq HCl, and the organic layer was separated, washed with saturated NaHCO₃ solution, and water, and freed from the solvent. The crude product was purified by recrystallization from a CH₂Cl₂/pentane mixture.

(E)-1,3-Bis(3-fluorophenyl)allyl 3,5-Dinitrobenzoate (1b-ODNB). From **1b-OH** (300 mg, 1.22 mmol), DNBCl (562 mg, 2.44 mmol), and Et₃N (350 μL, 2.54 mg, 2.51 mmol): 199 mg (0.451 mmol, 37%), yellowish powder (mp 130.0–131.5 °C). ¹H NMR (CDCl₃, 300 MHz): δ 6.48 (dd, ³J_{HH} = 15.9, 7.1 Hz, 1 H, ArCHCHCH(ODNB)-Ar), 6.67–6.79 (m, 2 H, ArCHCHCH(ODNB)Ar), ArCHCHCH(ODNB)Ar, 6.92–7.03 (m, 1 H, H_{Ar}), 7.03–7.36 (m, 6 H, H_{Ar}), 7.36–7.48 (m, 1 H, H_{Ar}), 9.18–9.22 (m, 2 H, H_{ODNB}), 9.22–9.25 ppm (m, 1 H, H_{ODNB}). ¹³C NMR (CDCl₃, 75 MHz): δ 78.1 (d, J_{CF} = 2.0 Hz, CH), 113.3 (d, J_{CF} = 22.0 Hz, CH), 114.1 (d, J_{CF} = 22.5 Hz, CH), 115.6 (d, J_{CF} = 21.4 Hz, CH), 116.0 (d, J_{CF} = 21.1 Hz, CH), 122.6 (s, CH), 122.7 (d, J_{CF} = 3.1 Hz, CH), 122.9 (d, J_{CF} = 2.9 Hz, CH), 126.6 (s, CH), 129.5 (s, CH), 130.2 (d, J_{CF} = 8.4 Hz, CH), 130.7 (d, J_{CF} = 8.2 Hz, CH), 133.7 (s, C), 133.8 (d, J_{CF} = 2.6 Hz, CH), 137.7 (d, J_{CF} = 7.7 Hz, C), 140.1 (d, J_{CF} = 7.1 Hz, C), 148.7 (s, C), 161.5 (s, C), 163.0 (d, J_{CF} = 247.5 Hz, C), 163.1 ppm (d, J_{CF} = 246.2 Hz, C). ¹⁹F NMR (CDCl₃, 282 MHz): δ -113.0 to -112.9 (m), -111.5 to -111.4 ppm (m). HRMS (EI+): calcd 440.0814 (C₂₂H₁₄F₂N₂O₆), found 440.0808.

(E)-1,3-Bis(4-bromophenyl)allyl 3,5-Dinitrobenzoate (1c-ODNB). From **1c-OH** (1.63 g, 4.43 mmol), DNBCl (1.03 g, 4.47 mmol), and Et₃N (750 μL, 545 mg, 5.38 mmol): 1.05 g (1.87 mmol, 42%), yellowish powder (mp 161.5–163.1 °C). ¹H NMR (CD₂Cl₂, 400 MHz): δ 6.51 (dd, ³J_{HH} = 15.9, 7.0 Hz, 1 H, ArCHCHCH(ODNB)-Ar), 6.68–6.74 (m, 2 H, ArCHCHCH(ODNB)Ar), ArCHCHCH(ODNB)Ar, 7.29–7.36 (m, 2 H, H_{Ar}), 7.40–7.50 (m, 4 H, H_{Ar}), 7.56–7.62 (m, 2 H, H_{Ar}), 9.18–9.19 (m, 2 H, H_{ODNB}), 9.21–9.22 ppm (m, 1 H, H_{ODNB}). ¹³C NMR (CD₂Cl₂, 101 MHz): δ 78.8 (CH), 122.9 (C), 123.2 (CH), 123.3 (C), 127.1 (CH), 128.9 (CH), 129.5 (CH), 130.1 (CH), 132.4 (CH), 132.6 (CH), 133.8 (CH), 134.3 (C), 135.2 (C), 137.7 (C), 149.3 (C), 162.2 ppm (C). HRMS (EI+): calcd 559.9213 (C₂₂H₁₄Br₂N₂O₆), found 559.9220.

(E)-1,3-Bis(4-chlorophenyl)allyl 3,5-Dinitrobenzoate (1d-ODNB). From **1d-OH** (1.08 g, 3.87 mmol), DNBCl (900 mg, 3.90 mmol), and Et₃N (650 μL, 472 mg, 4.66 mmol): 0.851 g (1.80 mmol, 47%), colorless powder (mp 150.0–151.5 °C). ¹H NMR (CD₂Cl₂, 400 MHz): δ 6.50 (dd, ³J_{HH} = 15.9, 7.0 Hz, 1 H, ArCHCHCH(ODNB)-Ar), 6.66–6.77 (m, 2 H, ArCHCHCH(ODNB)Ar), ArCHCHCH(ODNB)Ar, 7.29–7.35 (m, 2 H, H_{Ar}), 7.35–7.41 (m, 2 H, H_{Ar}), 7.41–7.46 (m, 2 H, H_{Ar}), 7.47–7.52 (m, 2 H, H_{Ar}), 9.18 (d, ³J_{HH} = 2.1 Hz, 2 H, H_{ODNB}), 9.22 ppm (t, ³J_{HH} = 2.1 Hz, 1 H, H_{ODNB}). ¹³C NMR (CD₂Cl₂, 101 MHz): δ 78.8 (CH), 123.2 (CH), 127.0 (CH), 128.7 (CH), 129.2 (CH), 129.4 (CH), 129.6 (CH), 130.1 (CH), 133.7 (CH), 134.4 (C), 134.7 (C), 134.8 (C), 135.2 (C), 137.2 (C), 149.3 (C), 162.2 ppm (C). HRMS (EI+): calcd 472.0223 (C₂₂H₁₄Cl₂N₂O₆), found 472.0225.

(E)-1,3-Diphenylallyl 3,5-Dinitrobenzoate (1e-ODNB). From **1e-OH** (1.00 g, 4.76 mmol), DNBCl (1.10 g, 4.77 mmol), and Et₃N (800 μL, 581 mg, 5.74 mmol): 731 mg (1.81 mmol, 38%), colorless powder (mp 154.1–155.5 °C). ¹H NMR (CDCl₃, 300 MHz): δ 6.52 (dd, ³J_{HH} = 16.0, 7.1 Hz, 1 H, PhCHCHCH(ODNB)Ph), 6.70–6.83 (m, 2 H, PhCHCHCH(ODNB)Ph), PhCHCHCH(ODNB)Ph, 7.23–7.48 (m, 8 H, H_{Ar}), 7.48–7.56 (m, 2 H, H_{Ar}), 9.15–9.25 ppm (m, 3 H, H_{ODNB}). ¹³C NMR (CDCl₃, 75 MHz): δ 79.3 (CH), 122.4 (CH), 125.9 (CH), 126.8 (CH), 127.1 (CH), 128.6 (CH), 128.7 (CH), 128.9 (CH), 129.0 (CH), 129.5 (CH), 134.1 (C), 134.5 (CH), 135.6 (C), 138.0 (C), 148.7 (C), 161.6 ppm (C). HRMS (EI+): calcd 404.1003 (C₂₂H₁₆N₂O₆), found 404.1005.

(E)-1,3-Di-p-tolylallyl 3,5-Dinitrobenzoate (1f-ODNB). From **1f-OH** (1.00 g, 4.20 mmol), DNBCl (968 mg, 4.20 mmol), and Et₃N (700 μL, 508 mg, 5.02 mmol): 900 mg (2.08 mmol, 50%), colorless powder (mp 84.5–86.0 °C). ¹H NMR (CD₂Cl₂, 400 MHz): δ 2.33 (s, 3 H, CH₃), 2.37 (s, 3 H, CH₃), 6.49 (dd, ³J_{HH} = 15.9, 7.2 Hz, 1 H, ArCHCHCH(ODNB)Ar), 6.66–6.76 (m, 2 H, ArCHCHCH(ODNB)Ar), ArCHCHCH(ODNB)Ar, 7.11–7.17 (m, 2 H, H_{Ar}), 7.22–7.28 (m, 2 H, H_{Ar}), 7.28–7.35 (m, 2 H, H_{Ar}), 7.40–7.46 (m, 2 H, H_{Ar}), 9.16–9.23 ppm (m, 3 H, H_{ODNB}). ¹³C NMR (CD₂Cl₂, 101

MHz): δ 21.48 (CH₃), 21.51 (CH₃), 80.0 (CH), 123.0 (CH), 125.8 (CH), 127.2 (CH), 127.7 (CH), 129.9 (CH), 130.0 (CH), 130.1 (CH), 133.6 (C), 134.4 (CH), 134.8 (C), 136.0 (C), 139.1 (C), 139.3 (C), 149.2 (C), 162.3 ppm (C). HRMS (EI+): calcd 432.1316 (C₂₄H₂₀N₂O₆), 432.1331.

1,3-Diaryllallyl 4-Nitrobenzoates (1-OPNB). 1-OPNB were obtained following the protocol described in ref 6.

(E)-1,3-Bis(4-bromophenyl)allyl 4-Nitrobenzoate (1c-OPNB). From **1c-OH** (1.00 g, 2.72 mmol), PNBCl (760 mg, 4.10 mmol), Et₃N (500 μL, 436 mg, 4.30 mmol), and DMAP (33.0 mg, 270 μmol): 477 mg (0.923 mmol, 34%), colorless powder (mp 130.7–132.0 °C). ¹H NMR (CD₂Cl₂, 400 MHz): δ 6.47 (dd, ³J_{HH} = 15.9, 6.7 Hz, 1 H, ArCHCHCH(OPNB)Ar), 6.63 (d, ³J_{HH} = 6.7 Hz, 1 H, ArCHCHCH(OPNB)Ar), 6.69 (d, ³J_{HH} = 15.9 Hz, 1 H, ArCHCHCH(OPNB)Ar), 7.25–7.34 (m, 2 H, H_{Ar}), 7.37–7.44 (m, 2 H, H_{Ar}), 7.44–7.51 (m, 2 H, H_{Ar}), 7.52–7.60 (m, 2 H, H_{Ar}), 8.23–8.34 ppm (m, 4 H, H_{OPNB}). ¹³C NMR (CD₂Cl₂, 101 MHz): δ 77.5 (CH), 122.7 (C), 123.0 (C), 124.2 (CH), 127.8 (CH), 128.9 (CH), 129.4 (CH), 131.4 (CH), 132.3 (CH), 132.5 (CH), 132.9 (CH), 135.5 (C), 136.0 (C), 138.3 (C), 151.3 (C), 164.2 ppm (C). HRMS (EI+): calcd 514.9362 (C₂₂H₁₅Br₂NO₄), found 514.9379.

(E)-1,3-Diphenylallyl 4-Nitrobenzoate (1e-OPNB). From **1e-OH** (200 mg, 951 μmol), PNBCl (180 mg, 970 μmol), Et₃N (160 μL, 116 mg, 1.15 mmol), and DMAP (20 mg, 164 μmol): 281 mg (782 μmol, 82%), colorless solid (mp 92.5–93.5 °C). The ¹H and ¹³C NMR spectra of **1e-OPNB** agreed with those described in ref 32.

(E)-1,3-Di-p-tolylallyl 4-Nitrobenzoate (1f-OPNB). From **1f-OH** (1.00 g, 4.20 mmol), PNBCl (1.01 g, 5.44 mmol), Et₃N (900 μL, 653 mg, 6.46 mmol), and DMAP (66.5 mg, 544 μmol): 727 mg (1.88 mmol, 45%), colorless powder (mp 92.6–94.0 °C). ¹H NMR (CDCl₃, 300 MHz): δ 2.35 (s, 3 H, CH₃), 2.37 (s, 3 H, CH₃), 6.43 (dd, ³J_{HH} = 15.9, 6.9 Hz, 1 H, ArCHCHCH(OPNB)Ar), 6.63–6.75 (m, 2 H, ArCHCHCH(OPNB)Ar), ArCHCHCH(OPNB)Ar, 7.07–7.18 (m, 2 H, H_{Ar}), 7.19–7.26 (m, 2 H, H_{Ar}), 7.27–7.33 (m, 2 H, H_{Ar}), 7.34–7.45 (m, 2 H, H_{Ar}), 8.24–8.31 ppm (m, 4 H, H_{OPNB}). ¹³C NMR (CDCl₃, 75 MHz): δ 21.19 (CH₃), 21.21 (CH₃), 78.0 (CH), 123.5 (CH), 125.8 (CH), 126.7 (CH), 127.1 (CH), 129.3 (CH), 129.4 (CH), 130.8 (CH), 133.1 (C), 133.4 (CH), 135.8 (C), 135.9 (C), 138.2 (C), 138.4 (C), 150.5 (C), 163.7 ppm (C). HRMS (EI+): calcd 387.1465 (C₂₄H₂₁NO₄), found 387.1482.

■ ASSOCIATED CONTENT

📄 Supporting Information

Details of the kinetic experiments, additional Hammett and Winstein–Grunwald correlations, and copies of the NMR spectra of new compounds. This material is available free of charge via the Internet at <http://pubs.acs.org>.

■ AUTHOR INFORMATION

✉ Corresponding Author

*E-mail: herbert.mayr@cup.uni-muenchen.de.

Notes

The authors declare no competing financial interest.

■ ACKNOWLEDGMENTS

We thank the Deutsche Forschungsgemeinschaft (Ma 673/22-1) for financial support. We are grateful to Anna Antipova, Johannes Ammer, and Dr. Armin R. Ofial for their help during preparation of this manuscript.

■ REFERENCES

(1) More precisely, the generation of the free ions from a covalent substrate should be termed as *ionization plus dissociation*: Reichardt, C.; Welton, T. *Solvents and Solvent Effects in Organic Chemistry*, 4th ed.; Wiley: Weinheim, 2011; p 52. To avoid the long terms, we used the term *heterolysis* as a description of this process.

(2) (a) Mayr, H.; Kempf, B.; Ofial, A. R. *Acc. Chem. Res.* **2003**, *36*, 66–77. (b) For a database of reactivity parameters E , N , and s_N see: www.cup.lmu.de/oc/mayr/DBintro.html, (last accessed on November 2, 2013).

(3) (a) Streidl, N.; Denegri, B.; Kronja, O.; Mayr, H. *Acc. Chem. Res.* **2010**, *43*, 1537–1549. (b) Denegri, B.; Streiter, A.; Jurić, S.; Ofial, A. R.; Kronja, O.; Mayr, H. *Chem.—Eur. J.* **2006**, *12*, 1648–1656; *Chem.—Eur. J.* **2006**, *12*, 5415. (c) Matić, M.; Jurić, S.; Denegri, B.; Kronja, O. *Int. J. Mol. Sci.* **2012**, *13*, 2012–2024. (d) Splitting up of the general nucleofugality scale described in refs 3a and 3b into separate scales for different types of electrofuges has been suggested: Bentley, T. W. *Chem.—Eur. J.* **2006**, *12*, 6514–6520.

(4) See, for instance: (a) Hughes, E. D. *Trans. Faraday Soc.* **1941**, *37*, 603–631. (b) Roberts, J. D.; Young, W. G.; Winstein, S. *J. Am. Chem. Soc.* **1942**, *64*, 2157–2164. (c) Young, W. G.; Winstein, S.; Goering, H. L. *J. Am. Chem. Soc.* **1951**, *73*, 1958–1963. (d) De La Mare, P. B. D.; Vernon, C. A. *J. Chem. Soc.* **1954**, 2504–2510. (e) Sneen, R. A. *J. Am. Chem. Soc.* **1960**, *82*, 4261–4269. (f) Jia, Z. S.; Ottosson, H.; Zeng, X.; Thibblin, A. *J. Org. Chem.* **2002**, *67*, 182–187. For a review, see: (g) Raber, D. J.; Harris, J. M.; Schleyer, P. v. R. in *Ions and Ion Pairs in Organic Reactions*; Szwarc, M., Ed.; Wiley: New York, 1974; Vol. 2.

(5) (a) Goering, H. L.; Blanchard, J. P.; Silversmith, E. F. *J. Am. Chem. Soc.* **1954**, *76*, 5409–5418. (b) Goering, H. L.; Silversmith, E. F. *J. Am. Chem. Soc.* **1955**, *77*, 1129–1133. (c) Goering, H. L.; Silversmith, E. F. *J. Am. Chem. Soc.* **1955**, *77*, 6249–6253. (d) Goering, H. L.; Takahashi Doi, J. *J. Am. Chem. Soc.* **1960**, *82*, 5850–5854. (e) Goering, H. L.; Nevitt, T. D.; Silversmith, E. F. *J. Am. Chem. Soc.* **1955**, *77*, 5026–5032. (f) Goering, H. L.; Koerner, G. S.; Linsay, E. C. *J. Am. Chem. Soc.* **1971**, *93*, 1230–1234.

(6) Troshin, K.; Mayr, H. *J. Am. Chem. Soc.* **2013**, *135*, 252–265.

(7) Troshin, K.; Schindele, C.; Mayr, H. *J. Org. Chem.* **2011**, *76*, 9391–9408.

(8) Streidl, N.; Antipova, A.; Mayr, H. *J. Org. Chem.* **2009**, *74*, 7328–7334.

(9) Horn, M.; Mayr, H. *J. Phys. Org. Chem.* **2012**, *25*, 979–988 and references therein.

(10) Minegishi, S.; Loos, R.; Kobayashi, S.; Mayr, H. *J. Am. Chem. Soc.* **2005**, *127*, 2641–2649.

(11) These values were reported for 50% aq acetonitrile (ref 2b); however, as the differences between the N values of 50% ($N = 5.05$, $s_N = 0.89$) and 80% ($N = 5.02$, $s_N = 0.89$) aq acetonitrile are marginal and the corresponding s_N values are equal, one would expect similar N and s_N values for 60% aq acetonitrile.

(12) (a) Grunwald, E.; Winstein, S. *J. Am. Chem. Soc.* **1948**, *70*, 846–854. (b) Bentley, T. W.; Carter, G. E. *J. Am. Chem. Soc.* **1982**, *104*, 5741–5747. (c) Kevill, D. N.; D'Souza, M. J. *J. Chem. Res.* **2008**, 61–66. The Y_{benzyl} parameters were taken from: (d) Bentley, T. W.; Dauschmidt, J.-P.; Llewellyn, G.; Mayr, H. *J. Org. Chem.* **1992**, *57*, 2387–2392.

(13) Winstein–Grunwald correlations for benzhydryl chlorides are based on the kinetic data from ref 3a and can be found in the Supporting Information.

(14) One reviewer raised the question of whether it is justified to use the Y_{benzyl} values (derived from 4-methoxybenzyl chloride solvolyses, ref 12d) for the correlations for 1-OPNB and 1-ODNB considering the availability of Y_{BnOPNB} scale (derived from solvolyses of 2-aryl-2-adamantyl 4-nitrobenzoates: Liu, K.-T.; Chang, C.-W.; Chen, H.-I.; Chin, C.-P.; Duann, Y.-F. *J. Phys. Org. Chem.* **2000**, *13*, 203–207; *J. Phys. Org. Chem.* **2000**, *13*, 306. In order to directly compare the effects of electrofuge and nucleofuge variation on m , it was crucial to use the same Y scale for all correlations. As the Y_{benzyl} scale provided the best correlations among the scales containing parameters for aqueous acetonitrile, we have chosen it as the basis for our analysis.

(15) Denegri, B.; Kronja, O. *J. Phys. Org. Chem.* **2009**, *22*, 495–503.

(16) Hansch, C.; Leo, A.; Taft, R. W. *Chem. Rev.* **1991**, *91*, 165–195.

(17) Streidl, N.; Mayr, H. *Eur. J. Org. Chem.* **2011**, 2498–2506.

(18) *What'sBest!7.0* (May 25, 2004) software by Lindo Systems, Inc., 2004, was used for this purpose.

(19) The values obtained at B3LYP/6-31G(d,p) level of theory were used, as they are available both for 1a–h (ref 7) and benzhydrylium ions: Singer, T. Dissertation, Ludwig-Maximilians-Universität, München, 2008.

(20) (a) Marcus, R. A. *Annu. Rev. Phys. Chem.* **1964**, *15*, 155–196. (b) Marcus, R. A. *J. Phys. Chem.* **1968**, *72*, 891–899. (c) Marcus, R. A. *J. Am. Chem. Soc.* **1969**, *91*, 7224–7225. (d) Albery, W. J.; Kreevoy, M. M. *Adv. Phys. Org. Chem.* **1978**, *16*, 87–157. (e) Albery, W. J. *Annu. Rev. Phys. Chem.* **1980**, *31*, 227–263. (f) Marcus, R. A. *Angew. Chem., Int. Ed. Engl.* **1993**, *32*, 1111–1121. (g) Marcus, R. A. *Pure Appl. Chem.* **1997**, *69*, 13–29.

(21) (a) Rice, F. O.; Teller, E. *J. Chem. Phys.* **1938**, *6*, 489–496. (b) Hine, J. J. *J. Org. Chem.* **1966**, *31*, 1236–1244. (c) Hine, J. J. *Am. Chem. Soc.* **1966**, *88*, 5525–5528. (d) Hine, J. *Adv. Phys. Org. Chem.* **1978**, *15*, 1–61.

(22) (a) Kantner, S. S.; Humski, K.; Goering, H. L. *J. Am. Chem. Soc.* **1982**, *104*, 1693–1697. (b) Thibblin, A. *J. Chem. Soc. Perkin. Trans.* **1987**, *2*, 1629–1632.

(23) A rationalization of this behavior by quantum chemical methods turned out to be unsuccessful as the predicted electrofugality parameters E_f for amino- and alkoxy-substituted benzhydrylium ions deviated significantly from the corresponding experimental values published almost simultaneously (ref 3a): Ormazábal-Toledo, R.; Camporodónico, P. R.; Contreras, R. *Org. Lett.* **2011**, *13*, 822–824.

(24) Phan, T. B.; Nolte, C.; Kobayashi, S.; Ofial, A. R.; Mayr, H. *J. Am. Chem. Soc.* **2009**, *131*, 11392–11401.

(25) Reichardt, C.; Welton, T. *Solvents and Solvent Effects in Organic Chemistry*, 4th ed.; Wiley: Weinheim, 2011; p 181.

(26) Gelles, E.; Hughes, E. D.; Ingold, C. K. *J. Chem. Soc.* **1954**, 2918–2929.

(27) Schaller, H. F.; Mayr, H. *Angew. Chem., Int. Ed.* **2008**, *47*, 3958–3961.

(28) Richard, J. P.; Jencks, W. P. *J. Am. Chem. Soc.* **1984**, *106*, 1383–1396.

(29) Nolte, C.; Mayr, H. *Eur. J. Org. Chem.* **2010**, 1435–1439.

(30) Troshin, K.; Mayer, P.; Mayr, H. *Organometallics* **2012**, *31*, 2416–2424.

(31) Hayashi, T.; Yamamoto, A.; Yoshihiko, I.; Nishioka, E.; Miura, H.; Yanagi, K. *J. Am. Chem. Soc.* **1989**, *111*, 6301–6311.

(32) Hollingworth, S.; Hazari, A.; Hopkinson, M. N.; Tredwell, M.; Benedetto, E.; Huiban, M.; Gee, A. D.; Brown, J. M.; Gouverneur, V. *Angew. Chem., Int. Ed.* **2011**, *50*, 2613–2617.